EXPERIMENTAL AND SIMULATION STUDY ON THE THERMAL-MECHANICAL PERFORMANCE OF PHASE CHANGE ENERGY PILE

by

Songying ZHAO[a*], Yifan ZHU[a], Kai XU[a], Hong CHANG[b], and Lei CHEN[a]

[a] School of Municipal and Environmental Engineering, Jilin Jianzhu University, Changchun, China
[b] School of Geomatics and Prospecting Engineering, Jilin Jianzhu University, Changchun, China

Original scientific paper
https://doi.org/10.2298/TSCI240630243Z

Phase change materials are incorporated into concrete to create phase change pile storage concrete, significantly enhancing the heat transfer efficiency of energy piles. However, adding these aggregates reduces concrete strength. This research examines how different proportions of steel balls, silicon carbide powder, and steel fibers affect the thermal and mechanical properties of pile foundation concrete. An orthogonal test under compressive design strength shows that a mix of 9% silicon carbide powder, 0.7% steel fiber, and 15% steel balls increases thermal conductivity by 25.3%. Numerical simulations with this optimized ratio indicate a 21% increase in heat transfer per unit depth compared to standard energy piles. The phase change energy pile notably lessens thermal effects on soil. Within 30 days of operation, its thermal influence radius decreased by 11.9%. Furthermore, maximum reductions in side friction, pile side stress, and displacement were recorded at 95.9%, 59.1%, and 80.3%, respectively, demonstrating excellent structural stability.

Key words: *phase change materials, energy pile, enhance heat transfer, mechanical properties*

Introduction

Geothermal energy is acclaimed as a renewable resource with substantial potential [1]. The energy pile system, an innovative structural element, doubles as a foundation and a conduit for geothermal energy transfer into buildings via embedded heat exchange tubes. Hamada's [2] field studies on friction piles as subterranean heat exchangers affirm the system's efficacy in space heating and cooling, and its role in curtailing primary energy use and GHG emissions. Recent efforts to boost energy pile heat transfer efficiency have focused on design parameters [3], pipe-line configurations [4-6], groundwater flow rates [7, 8], and operational modes [9, 10]. Nowadays great progress has been made in these studies, however, significant bottlenecks are still remained. The long-term operation of energy pile systems leads to thermal interference among heat exchange tubes and thermal accumulation in the soil, reducing the overall heat exchange performance of the system [11].

The efficiency of energy pile systems largely depends on the thermal exchange capacity of concrete [12]. The PCM are ideal for enhancing this capacity due to their ability to absorb or release significant latent heat during phase changes [13]. Currently, PCM are widely used in engineering and can significantly improve the heat exchange efficiency of energy piles [14-18].

* Corresponding author, e-mail: zhaosongying@jlju.edu.cn

Research by Chang *et al.* [19] showed that phase change energy piles (PCEP) made with PCM can increase heat transfer efficiency by up to 46.8% compared to ordinary energy piles (OEP), with minimal impact on surrounding soil. However, selecting suitable PCM and their combinations to enhance heat transfer while maintaining or improving compressive strength are still considered as a key challenge in current research.

Scholars have extensively studied PCM selection and combinations. Kong *et al.* [20] used graphite in reinforced concrete, increasing the heat transfer coefficient by 66.1% and improving heat transfer efficiency by 6.5%. Several important key challenges and issues on the way to advanced graphite anodes with superior rate/capacity/cycle performance are discussed by Zhang *et al.* [21]. But Li *et al.* [22] noted potential structural performance reduction. Paraffin wax, an ideal heat storage material, boosts thermal conductivity when combined with graphite [23, 24], but leakage risks require suitable encapsulation. Cui *et al.* [25] introduced a PCEP based on paraffin wax, reducing thermal stress, while Dong *et al.* [26] encapsulated PCM in hollow steel balls (HSB) for concrete, mitigating leakage but facing bearing capacity challenges. Research has emerged on combining PCM with additives to create composite materials, such as incorporating steel fibers to enhance thermal conductivity and mechanical strength [27, 28]. Silicon carbide powder (SiC) improves concrete's heat storage and mechanical properties [29, 30], enhancing heat transfer and compressive strength in energy piles [22]. However, limited research exists on the comprehensive effects of composite PCM like graphite, paraffin wax and SiC, particularly with specific encapsulation methods and additives.

In summary, PCM shows promise in improving concrete's heat storage and energy piles' efficiency and mechanics, since further study on its specific use and overall impact in energy piles are still needed. This research focuses on experimentally optimizing composite materials, ratios, and packaging for energy piles. A heat transfer and thermo-mechanical model uses simulation compare PCM-reinforced energy piles with OEP. Integrating PCM aims to enhance thermal storage and heat exchange, while combining additives with composite PCM seeks to reduce structural degradation. This research provides a scientific basis for applying PCM in energy piles.

Preparation and thermal and mechanical properties testing of pile block

Composition ratio and preparation of composite PCM

Ratio of mass fraction

In fabricating PCM-concrete, the initial step is assessing heat transfer and storage through physical tests to determine optimal material ratios. The composite PCM preparation involves controlling graphite addition avoid excessive amounts, adjusting SiC content for balance [22], and increasing paraffin for improved latent heat [31]. Specific ratios are detailed in tab. 1. Each material is weighed in accordance with the proportioning scheme. During the preparation process, paraffin is initially heated to the liquid state, followed by the addition of SiC and thorough stirring for 30 minutes to ensure uniform mixing. Subsequently, pre-dried expanded graphite is added and continuous stirring is carried out for 1 hour, eventually obtaining the composite PCM that meets the requirements.

Physical property testing and packaging

To evaluate heat transfer, the Hot Disk thermal constant analyzer is used, detailed in fig. 1(a). The 5501 probe (radius 6.403 mm, conductivity limit 100 W/mK) measures solid powder samples' thermal conductivity. Samples are compacted in a stainless steel container for probe contact, of which three samples per group are tested, with the average representing the group's

thermal conductivity. This study employs differential scanning calorimeter (DSC) to analyze composite PCM's thermophysical properties, with principles and set-up shown in fig. 1(b). DSC tests yields parameters like transition temperatures and latent heat for each material group.

Table 1. Different mass fraction ratios of PCM

Number	Paraffin [%]	Graphite [%]	SiC [%]	Number	Paraffin [%]	Graphite [%]	SiC [%]
A1	65	5	30	C1	65	15	20
A2	70	5	25	C2	70	15	15
A3	75	5	20	C3	75	15	10
A4	80	5	15	C4	80	15	5
B1	65	10	25	D1	65	20	15
B2	70	10	20	D2	70	20	10
B3	75	10	15	D3	75	20	5
B4	80	10	10	D4	80	20	0

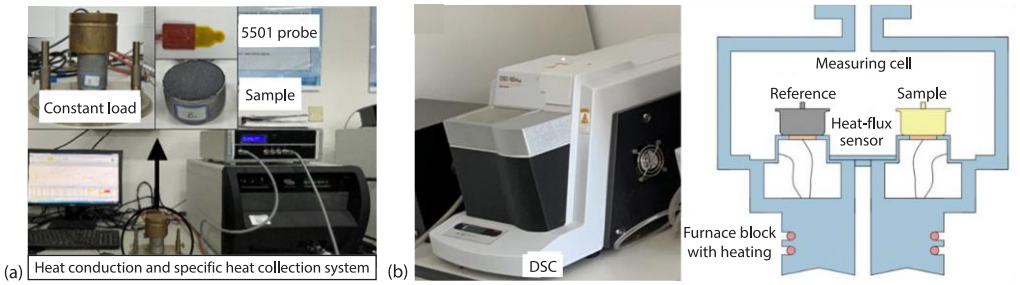

Figure 1. Hot Disk thermal constant test system and DSC

Figure 2(a) depicts paraffin's solid-to-liquid transition between 44 °C and 61 °C, absorbing substantial latent heat. Figure 2(b) summarizes test results for 16 composite PCM groups, with Group D3 showing higher thermal conductivity, latent heat, and specific heat. Increased graphite in paraffin boosts heat transfer and storage, making Group D3 the optimal choice for filling the HSB.

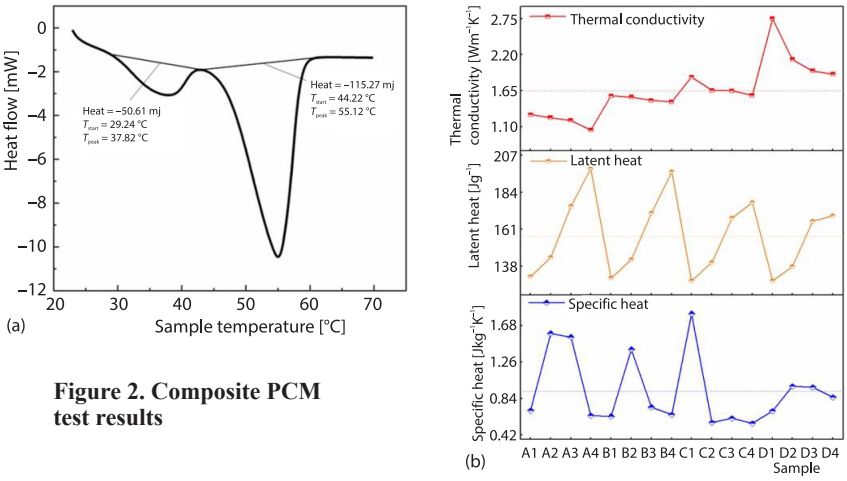

Figure 2. Composite PCM test results

The HSB is used to package D3 group materials, with detailed specifications listed in tab. 2. The packaging steps and required tools for the HSB are shown in fig. 3. During packaging, rivets, washers and AB glue ensure stability and sealing.

Table 2. Specifications of phase change steel balls – PCSB

Materials	Model	Specification
HSB	Stainless steel 304	Φ_1 = 19 mm, d_1 = 1 mm
Rivet	Aluminum flat head	Φ_2 = 3 mm, l_1 = 5 mm
Gasket	Stainless steel 304	Φ_3 = 6 mm, Φ_4 = 3 mm, d_2 = 1 mm
Sealant	Acrylic blue-red AB glue	

Figure 3. The PCSB package

A random sample of 50 punched, non-encapsulated HSB is weighed, whereas encapsulated PCSB underwent double weighing. Adsorption rate (38.90% for PCM by HSB) is determined using eq. (1), and density (1.44 kg/m³) is calculated using eq. (2). To evaluate PCSB impermeability, they are subjected to 10 cycles in an electrothermal drying box at 80 °C and an incubator at 0 °C, followed by weighing. Equation (3) is then used to calculate a low leakage rate of 0.26%. These results highlight encapsulation's effectiveness in enhancing PCSB sealing and minimizing PCM leakage during phase changes, making this method suitable for PCC preparation:

$$P_1 = \frac{m_1 - m_0}{m_0} \times 100\% \tag{1}$$

$$\rho = \frac{m_1}{50V} \times 100\% \tag{2}$$

$$P_2 = \frac{m_1 - m_2}{m_1} \times 100\% \tag{3}$$

where P_1 [%] is the adsorption rate of PCM, m_0 [g] – the total mass of 50 HSB, m_1 [g] – the total mass of 50 PCSB, P_2 [%] – the leakage rate of PCM, m_2 [g] – the total mass of 50 PCSB after leakage test, and ρ [kgm^{-3}] – the density of PCSB, and V [m^3] – the volume of HSB.

Proportion and preparation of pile block

This study uses P·O 42.5 Portland cement from *Jilin Yatai Dinglu Cement Co., Ltd*, basalt sand (5-20 mm), and medium sand (fineness modulus 2.76) to prepare C45 pile foun-

dation concrete blocks per *GB50010-2010*. Aggregate amounts are determined using eqs. (4) and (5), recognizing their direct impact on performance. PCSB, steel fibers and SiC partially replace coarse aggregate in preparing the test blocks:

$$\frac{m_{c0}}{\rho_c}+\frac{m_{g0}}{\rho_g}+\frac{m_{s0}}{\rho_s}+\frac{m_{w0}}{\rho_w}+0.01\alpha=1 \tag{4}$$

$$\beta_s=\frac{m_{s0}}{m_{g0}-m_{s0}}\times 100\% \tag{5}$$

where m_{c0} [kg] is the cement mass, m_{g0} [kg] – the mass of coarse aggregate, m_{s0} [kg] – the mass of fine aggregate, m_{w0} [kg] – the mass of water, ρ_c [kgm^{-3}] – the cement density, ρ_g [kgm^{-3}] – the coarse aggregate density, ρ_w [kgm^{-3}] – the density of water, and β_s [%] – the sand rate.

Concrete mix ratio of pile foundation

Pre-tests reveals that PCSB's surface smoothness reduces cohesive force, setting a 50% upper limit for addition (0%, 15%, 30%, 45%) to ensure strength. SiC and steel fiber are varied (0-1% for steel fiber, 0-9% for SiC) to study their effects on heat transfer and mechanical properties. Using an orthogonal design, factors like SiC, steel fiber and PCSB content are selected, with the lowest effect term as an error term. Mixing these materials into concrete while adjusting other parameters (constant water-binder ratio) met design and construction requirements. The concrete incorporating phase change materials (PCC) mix ratio is shown in tab. 3.

Table 3. Mix ratio of PCC

Group number	Water [kg]	Cement [kg]	Sand [kg]	Gravel [kg]	SiC [kg]	Steel fiber [kg]	PCSB [pieces]
1	2.111	5.414	5.413	8.757	0.000	0.000	0
2	2.111	5.414	5.972	8.035	0.000	0.073	21
3	2.111	5.414	5.963	7.603	0.000	0.127	42
4	2.111	5.414	5.953	7.175	0.000	0.182	138
5	2.111	5.252	5.447	8.414	0.162	0.000	22
6	2.111	5.252	5.822	8.201	0.162	0.073	0
7	2.111	5.252	5.814	7.044	0.162	0.127	136
8	2.111	5.252	5.805	7.358	0.162	0.182	40
9	2.111	5.089	5.805	8.653	0.325	0.000	48
10	2.111	5.089	5.705	6.949	0.325	0.073	134
11	2.111	5.089	5.696	7.977	0.325	0.127	0
12	2.111	5.089	5.688	7.563	0.325	0.182	20
13	2.111	4.927	5.322	7.446	0.487	0.000	143
14	2.111	4.927	5.587	7.159	0.487	0.073	39
15	2.111	4.927	5.578	7.458	0.487	0.127	20
16	2.111	4.927	5.570	7.752	0.487	0.182	0

Preparation of pile foundation concrete test block

To ensure test accuracy and minimize errors, 16 groups of test blocks, each containing 6 blocks, were prepared. Thermal conductivity tests follow *ASTM C177-13*, and compressive

strength specimens are prepared per *BS EN 12390*. Three pieces measuring (300 mm × 300 mm × 30 mm) are used for thermal conductivity, while another three pieces measuring (100 mm × 100 mm × 100 mm) are used for compressive strength. Preparation involved weighing materials, pre-mixing PCSB and crushed stones, adding steel fibers, followed by cement and SiC for dry mixing. Water is added in three-stages for wet mixing. The mixture is filled into the mold in two layers, each vibrated, leveled, labeled and left indoors for 48 hours. After, it was placed in a curing box at 293K and 90% humidity. Performance tests are conducted after 28 days.

Thermal and mechanical properties test

Thermal conductivity is measured with the NETZSCH HFM-446 heat flowmeter, fig. 4(a). The test block is placed between temperature-adjustable plates, and heat flux power is calculated using the Fourier equation. A constant 20 °C temperature difference is maintained between the plates, and three samples from each group are tested for reliability. Since the composite PCM transitions between 44 °C and 61 °C, a specific test temperature of 50 °C is set (with the upper plate at 60 °C and the lower plate at 50 °C) to investigate its effect on the test block, as shown in fig. 4(b). Compressive performance is evaluated by using a YAR-2000 electro-hydraulic servo pressure tester, fig. 4(c), with load-displacement and deformation data recorded. Errors are minimized but not eliminated due to equipment accuracy, operational variations, and material property uncertainties. Relative tolerances are set at ±0.3% for the thermal conductivity tester and ±1.0% for the compression machine.

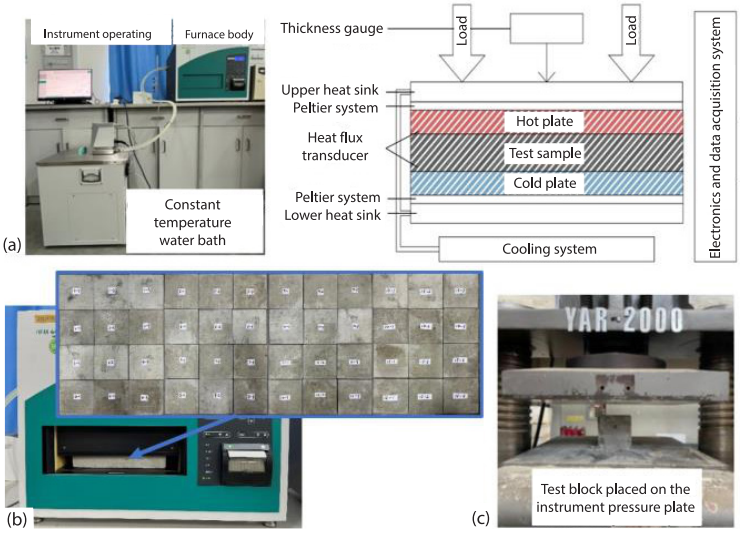

Figure 4. (a) Thermal conductivity test bench, (b) operation of thermal conductivity test, and (c) compressive strength test bench

Thermal properties

Research results indicate that all three materials enhanced thermal conductivity, with varying degrees of improvement. Range analysis of orthogonal test results showed ranges of 0.13 W/mK for SiC, 0.02 W/mK for steel fibers, and 0.06 W/mK for PCSB, directly correlating with their influence. Variance analysis, with F values of 18, 0.94, and 3.06, which fimly supports these findings.

Figure 5(a) shows that SiC content significantly impacts the thermal conductivity of pile foundation test blocks. As content rises from 0% to 3%, thermal conductivity increases rapidly by 10.64%, attributed to SiC's high thermal conductivity. Further increases to 6% slow the rate, but it accelerates again at 9%, indicating tighter interactions among SiC particles at higher concentrations. Figure 5(b) illustrates that PCSB positively correlates with the thermal conductivity of pile foundation concrete. Their internal phase-change process regulates material thermal conductivity within a specific temperature range. Thermal conductivity slightly increases from 0%-15% PCSB content, with a significant increase to 0.53 W/mK at 30%, representing an 8.16% rise. Beyond 30% to 45%, the growth rate decelerates, resulting in a final thermal conductivity of 0.55 W/mK. Figure 5(c) shows that steel fiber quantity has a minimal impact on thermal conductivity, with a relatively stable increase as content rises from 0%-0.7%. However, at 1% steel fiber content, there is a notable increase in thermal conductivity to 0.52 W/mK. Although steel fibers have lower thermal conductivities than SiC and PCSB, their unique structure enhances overall performance by facilitating continuous paths for heat transfer within the material.

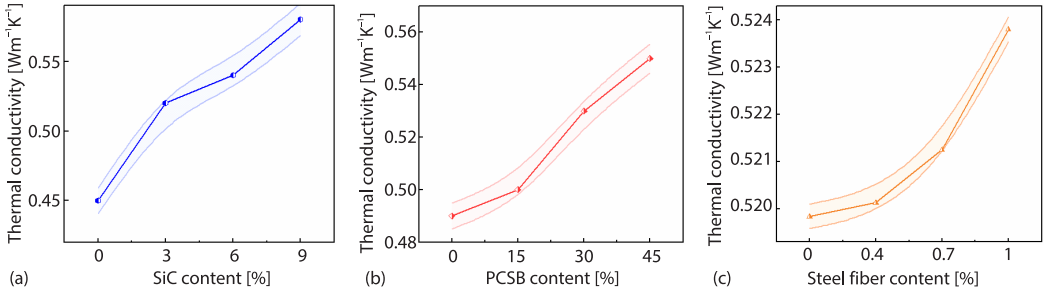

Figure 5. Influence on thermal conductivity; (a) SiC, (b) PCSB, and (c) steel fiber

Mechanical properties

To comprehend the impacts of SiC, steel fibers and PCSB on the mechanical properties of pile foundation test blocks, range analysis was conducted. The results indicated ranges of 2.52 MPa for SiC, 0.46 MPa for steel fibers, and 14.24 MPa for PCSB, highlighting PCSB's significant influence. This observation correlates with variance analysis, yielding F values of 0.74, 0.70, and 8.50, respectively for each material.

As shown in fig. 6(a), the compressive strength of the pile foundation test block increases with SiC content, rising significantly to 47.48 MPa at 6% and further to 48.21 MPa at 9%, a 5.5% increase from the 0% baseline. This significant increase indicates that adding SiC has improved the cohesion of concrete aggregates, enhancing the compressive strength of the test block. Figure 6(b) shows a negative correlation between the quantity of PCSB and the pile foundation test block's compressive strength. As dosage increases, particularly from 0% to 15%, compressive strength decreases noticeably. The downward trend slows as the blend volume increases to 30%, with a sharp drop to 39.35 MPa, a 19.6% decrease. It is due to the PCSB's smooth surface, which reduces friction with concrete aggregate, leading to decreased compressive strength. As illustrated in fig. 6(c), steel fibers positively impact the compressive strength of concrete specimens. A slight strength increase is observed from 0-0.4%, reaching 46.79 MPa, further rising to 46.90 MPa at 0.7% dosage, and peaking at 47.15 MPa at 1% dosage. This outcome indicates that an adequate amount of steel fibers can restrict crack propagation, enhancing compressive strength.

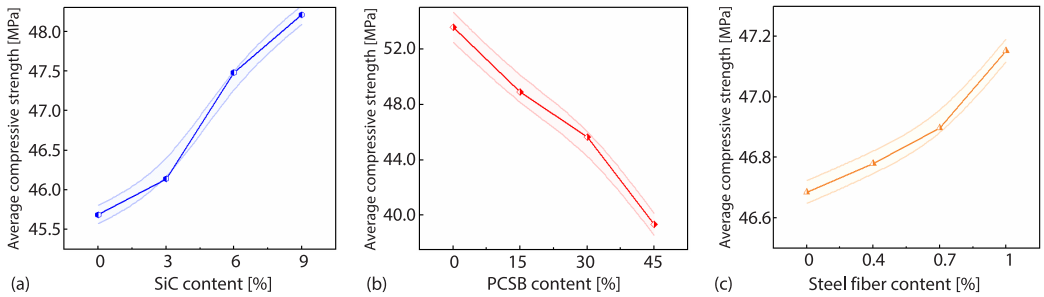

Figure 6. Influence on compressive strength; (a) SiC, (b) PCSB, and (c) steel fiber

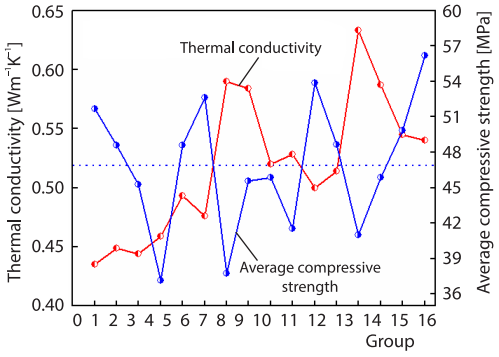

Figure 7. Thermal conductivity and compressive strength test results

Comprehensive analysis

Through using the comprehensive scoring method [32] with entropy-determined weights (52% for compressive strength, 48% for thermal conductivity), key variable influences were analyzed, excluding the PCSB-free group. Group 15, with 9% SiC, 0.7% steel fibers and 15% PCSB, was optimal. Figure 7 reveals that SiC enhances concrete's thermal conductivity, while PCSB impacts internal temperature and heat transfer. The combination of SiC and steel fibers counteracts potential PCSB drawbacks and boosts compressive strength. Group 15 balanced both properties, outperforming PCM-free blocks by 25.29% in thermal conductivity while maintaining above average compressive strength, aligning with scoring results.

Performance simulation of PCEP

Thermal properties

Physical model

Heat transfer simulations between energy piles and soil are complex, requiring assumptions: constant soil and material properties within 278-323 K, uniform fluid-flow and temperature on cross-sections, and negligible underground seepage [33]. Simulations compare a standard pile foundation (Group 1) with a PCEP (Group 15), using constant thermophysical parameters. The PCEP's latent heat is 1800 J/kg, see tab. 4 for other parameters. Figure 8(a) shows the energy pile's physical model. Grid cells vary by need: dense grids in pipe-lines and

Table 4. Material thermal property parameters

Material	Density [kgm^{-3}]	Thermal conductivity [Wm^{-1}K^{-1}]	Specific heat [Jkg^{-1}K^{-1}]
Soil	1800	1.8	1600
Common concrete	2214	0.435	1200
PCC	2235	0.545	1230
Pipe	950	0.42	2300
Water	998	0.6	4182

pile foundations, sparse at the soil mass edge. The heat exchange pipe-line has 5792161 grid elements, and the pile-soil part has 1900745, fig. 8(b). This simulation aims to compare the heat transfer performance of OEP and PCEP operating continuously for 30 days in winter. The inlet water temperature is set at 323 K with a flow velocity of 0.5 m/s, and both the initial soil and pile temperatures are kept at 293 K. The turbulence state simulation uses the standard k-ε model, with a turbulence intensity of 5%. The SIMPLE algorithm solves pressure-velocity coupling. A 3-D double-precision solution enhances accuracy.

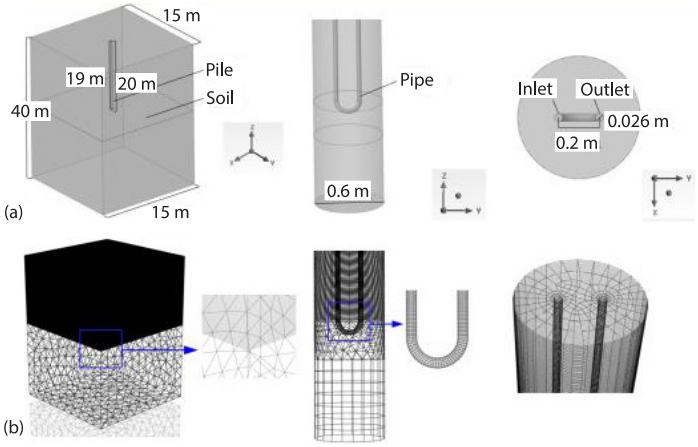

Figure 8. Heat transfer simulation pretreatment; (a) physical model and (b) meshing fraction

Thermal performance analysis

Figure 9(a) shows the thermal influence radius at a 10 m pile depth after 1, 7, 15, and 30 days for both energy pile systems. As operation continues, the thermal influence radius of both piles increases similarly, with heat transferring from water to the heat exchange tube, pile foundation, and soil. Initially (1 day), the radius differs by 0.01 m between systems. After 30 days, this difference grows to 0.21 m due to the PCEP's hysteresis effect. The PCEP has a slower heat diffusion rate than the OEP, indicating its thermal storage advantage. This agrees with Bao *et al.* [34]. Figure 9(b) shows that heat exchange increases the internal temperature, causing the PCM to absorb heat and transition a liquid state (0.48 liquid phase ratio after 30 days). It slows heat transfer and reduces diffusion surrounding soil, enhancing the pile foundation's thermal performance. As depicted in fig. 9(c), the PCEP consistently outperforms the OEP in thermal exchange efficiency, with a maximum increase of 21%. This advantage is attributed to the latent heat of phase change absorbed by the pile foundation material, which boosts its energy density and enhances the thermal exchange rate [35]. Figure 9(d) presents the temperature distribution curve at a 10 m depth, centered around the pile axis. The temperature in the pile foundation (highlighted area) is significantly higher than in the surrounding soil, with the difference increasing closer to the pile. Initially, the soil temperature around the OEP is higher than around the PCEP, and this disparity widens over time. For instance, at line 1 (x = –0.34 m), the OEP is 0.52K hotter than the PCEP after 1 day, 1.01K hotter after 7 days, and 1.28 K hotter after 30 days, albeit with a slowing growth rate.

The PCM enhance heat transfer within pile foundations while mitigating thermal impacts on the surrounding soil. This reduction in thermal effects on the soil helps alleviate soil

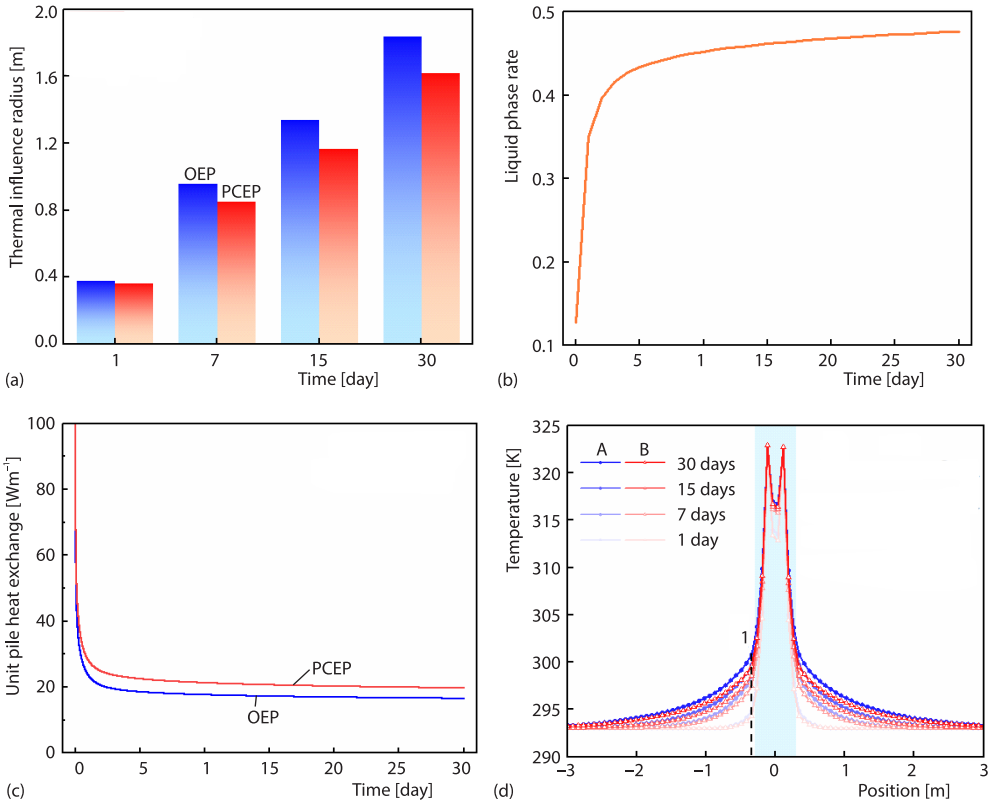

Figure 9. (a) Thermal influence radius, (b) phase change ratio of pile foundation, (c) heat transfer per unit pile depth, and (d) temperature distribution curve around pile (A: OEP, B: PCEP)

thermal accumulation. As a result, PCEP minimizes thermal interference with other piles, offering significant advantages in heat transfer performance.

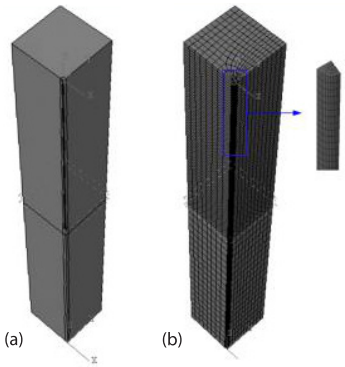

Figure 10. Thermal coupling simulation pretreatment

Mechanical properties

Thermo-mechanical coupled model

Due to the symmetrical geometry and load, the thermo-mechanical coupling model is simplified to a quarter of the pile-soil system, aligning with the heat conduction model's structural parameters, fig. 10(a). This model captures the pile foundation-soil interaction, representing heat transfer through interface thermal conductivity and shear force via frictional contact. The top allows free vertical displacement, while the bottom and sides are constrained. The grid configuration, fig. 10(b), employs an eight-node linear heat transfer hexahedron element (DC3D8 grid) and an eight-node linear hexahedron element (C3D8R grid) for coupling analysis. The grid division optimizes computational efficiency and

accuracy, using varying grid densities in different regions to capture temperature and stress gradients, respectively and precisely. Material properties are based on Liu *et al.* [36] test data, tab. 5. Predefined fields include temperatures of piles and soil after 15 and 30 days for 2 pile heat exchangers, with nodal temperatures imported from a heat transfer model before sequential coupling thermal stress analysis.

Table 5. Material characteristic parameter

Mechanical and thermal parameters	PCC	Common concrete	Soil
Elastic modulus [MPa]	35000	35500	20
Poisson's ratio [–]	0.25	0.25	0.28

Mechanical properties analysis

Figure 11(a) shows the variation in side friction resistance of two energy piles (PCEP and OEP) with depth over 15 and 30 days. Initially, PCEP has slightly higher lateral friction due to lower compressive strength. Over time, both piles show an increase tendency in side friction resistance, but PCEP's change is less (up to 0.99 kPa less), which indicates that it enhanced safety under extended temperature loading. Figure 11(b) illustrates the pile stress variation with depth, with negative values denoting compressive stresses. Stress is lower at the pile foundation's top and bottom, and higher in the middle. Compared to OEP, PCEP significantly reduced the stress difference variation by up to 59.1%, as indicated by the marked points in fig. 11(b). As depicted in fig. 11(c) from 15-30 days of operation, the OEP's displacement change is greater than that of the PCEP, with a reduction in displacement change of 0.06 mm. Hence, the incorporation of PCM enhances the pile foundation's structural stability.

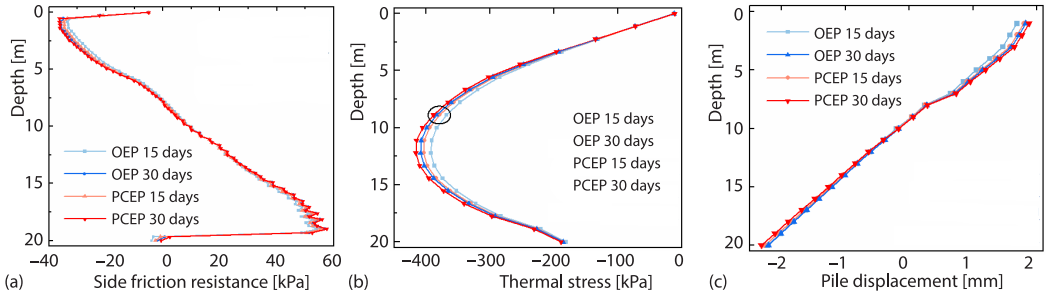

Figure 11. (a) Side friction resistance, (b) thermal stress, and (c) pile displacement

Conclusions

In order to enhance the heat transfer and compressive performance of the pile foundation, a composite PCM is added to the pile foundation material to prepare the phase change pile foundation test block. The thermal and mechanical properties of the PCEP and OEP are analyzed and compared through numerical simulation of heat transfer and thermal-mechanical coupling between the two piles. The main conclusions are as follows.

- The addition of SiC and PCSB enhances thermal conductivity, while SiC and steel fibers boost compressive strength in pile foundation test blocks. Balancing these properties is critical; the optimal mix ratio is 9% SiC, 15% PCSB and 0.7% steel fibers. This mix achieves a 25.3% increase in thermal conductivity while meeting design compression strength.

- Compared to OEP, PCEP shows significant improvement in heat exchange efficiency, with a 21% increase per pile depth. It mitigates heat impact on soil, alleviates soil heat accumulation, and slows heat diffusion between pile foundation and soil. After 30 days, PCEP's hysteresis effect reduces the heat influence radius by 0.21 m compared to OEP, and the liquid phase rate of PCM reaches 0.48.
- The PCEP demonstrates enhanced structural stability and improved mechanical properties over time. After 15 and 30 days of operation, PCEP showed significant reductions in side friction resistance (95.9%), pile stress (59.1%), and displacement (80.3%) compared to OEP.

Acknowledgment

This paper was made possible thanks to the generous support of the Science and Technology Department, Jilin Province (Grant No. 20230203115SF).

Nomenclature

DSC – differential scanning calorimeter
HSB – hollow steel balls
OEP – ordinary energy piles
PCC – concrete incorporating phase change materials
PCEP – phase change energy piles
PCSB – phase change steel balls
SiC – silicon carbide powder

References

[1] Shortall, R., *et al*., Geothermal Energy for Sustainable Development: A Review of Sustainability Impacts and Assessment Frameworks, *Renewable and Sustainable Energy Reviews*, *44* (2015), Apr., pp. 391-406
[2] Hamada, Y., *et al.*, Field Performance of an Energy Pile System For Space Heating, *Energy & Buildings*, *39* (2006), 5, pp. 517-524
[3] Bozis, D., *et al.*, On the Evaluation of Design Parameters Effects on the Heat Transfer Efficiency of Energy Piles, *Energy & Buildings*, *43* (2010), 4, pp. 1020-1029
[4] Zhao, Q., *et al*., Study on the Thermal Performance of Several Types of Energy Pile Ground Heat Exchangers: U-Shaped, W-Shaped and Spiral-Shaped, *Energy & Buildings*, *133* (2016), Dec., pp. 335-344
[5] Luo, J., *et al*., Thermo-Economic Analysis Of Four Different Types Of Ground Heat Exchangers In Energy Piles, *Applied Thermal Engineering*, *108* (2016), Sept., pp. 11-19
[6] Chang, H., *et al*., Study on the Thermal Response of Spiral Energy Piles Based on Field Test, *Thermal Science*, *27* (2023), 1A, pp. 195 - 205
[7] You, T.,.Yang, H., Influences of Different Factors on the 3-D Heat Transfer of Spiral-Coil Energy Pile Group with Seepage, *International Journal of Low-Carbon Technologies*, *15* (2020), 3, pp. 458-470
[8] Zhang, W., *et al.*, The Influence of Groundwater Seepage on the Performance of Ground Source Heat Pump System with Energy Pile, *Applied Thermal Engineering*, *162* (2019), C, pp. 114217-114217
[9] Tian, Y., Weitao, Z., Zoning Operation of Energy Piles to Alleviate the Soil Thermal Imbalance of Ground Source Heat Pump Systems, *Energy and Built Environment*, *4* (2023), 1, pp. 57-63
[10] Xu, B., *et al*., Study on Heat Transfer Performance of Geothermal Pile-Foundation Heat Exchanger with 3-U Pipe Configuration, *International Journal of Heat and Mass Transfer*, *147* (2020), Feb., pp. 119020-119020
[11] Park, S., *et al*., Effect of Thermal Interference on Energy Piles Considering Various Configurations of Heat Exchangers, *Energy & Buildings*, *199* (2019), Sept., pp. 381-401
[12] Qingwen, L., *et al*., Enhancing Heat Transfer in the Heat Exchange Medium of Energy Piles, *Journal of Building Engineering*, *40* (2021), 102375
[13] Barbi, S., *et al*., Phase Change Material Evolution in Thermal Energy Storage Systems for the Building Sector, with a Focus on Ground-Coupled Heat Pumps, *Polymers (Basel)*, *14* (2022), 3, 620
[14] Liang, M., Thermal Performance Experiment and Numerical Simulation of Micro-PCM Cement Mortar Composite Wall, *Thermal Science*, *27* (2023), 4A, pp. 3013-3028
[15] Ganbin, L., *et al*., Experiment and Simulation on Thermodynamic Characteristics of Phase Change Stee-Ball Concrete Energy Pile (in Chinese), *Journal of Hunan University (Natural Sciences)*, *50* (2023), 11, pp. 136-146

[16] Li, X., *et al*., Research on *U*-Tube Heat Exchanger with Shape-stabilized Phase Change Backfill Material, *Procedia Engineering*, *146* (2016), Dec., pp. 640-647
[17] Liu, Z., *et al.*, Application of Phase Change Energy Storage in Buildings: Classification of Phase Change Materials and Packaging Methods, *Thermal Science*, *26* (2022), 5B, pp. 4315-4332
[18] Zhang, X., *et al*., Numerical Simulation of Heat-Storage Performance of Filling Body with Uniformly Mixed Phase Change Paraffin, *Thermal Science*, *27* (2023), 6A, pp. 4609 - 4624
[19] Chang, H., *et al*., Experimental Study of Phase Change Energy Pile Based on Gum Arabic and Polyethylene Glycol 600 under Multiple Thermal-Cold Cycles, *Construction and Building Materials*, *438* (2024), 137109
[20] Kong, L.-P., *et al*., A Study on Heat Transfer Characteristics and Pile Group Influence of Enhanced Heat Transfer Energy Piles, *Journal of Building Engineering*, *24* (2019), 100768
[21] Zhang, H., *et al*., Graphite as Anode Materials: Fundamental Mechanism, Recent Progress and Advances, *Energy Storage Materials*, *36* (2021), Apr., pp. 147-170
[22] Li, Q., *et al*., Enhancing Heat Transfer in the Heat Exchange Medium of Energy Piles, *Journal of Building Engineering*, *40* (2021), 102375
[23] Kousksou, T., *et al*., Paraffin Wax Mixtures as Phase Change Materials, *Solar Energy Materials and Solar Cells*, *94* (2010), 12, pp. 2158-2165
[24] Lu, B., *et al*., Experimental investigation on Thermal Properties of Paraffin/Expanded Graphite Composite Material for Low Temperature Thermal Energy Storage, *Renewable Energy*, *178* (2021), Nov., pp. 669-678
[25] Cui, H., *et al.*, Experimental Study on Thermo-Mechanical Behavior of a Novel Energy Pile with Phase Change Materials Using Fiber Bragg Grating Monitoring, *Sustainability*, *16* (2023), 1, 206
[26] Dong, Z., *et al*., Development of Hollow Steel Ball Macro-Encapsulated PCM for Thermal Energy Storage Concrete, *Materials*, *9* (2016), 1, 59
[27] Yan, J. B., Gao, S., Experimental Study on Heat Transfer Enhancement of Heat Storage Material for Energy Pile, *Thermal Science*, *27* (2023), 1B, pp. 591-597
[28] Cui, H., *et al*., Study on the Thermal and Mechanical Properties of Steel Fibre Reinforced PCM-HSB Concrete for High Performance in Energy Piles, *Construction and Building Materials*, *350* (2022), 128822
[29] Kim, H. G., *et al*., Assessment of PCM/SiC-Based Composite Aggregate in Concrete, *Energy Storage Performance*, *258* (2020), 119637
[30] Bahari, A., *et al.*, Modification of Portland Cement with NanoSiC, Proc. Natl. Acad. Sci., India, Sect. A, *Phys. Sci*., *86* (2016), Jan., pp. 323-331
[31] Yu, R., *et al.*, Study on Preparation and Heat Transfer Enhancement of Expanded Graphite/Paraffin Composites, *Journal of Physics: Conference Series*, *2671* (2024), 012021
[32] Juchun, T., Jianmin, W., New Study on Determining the Weight of Index in Synthetic Weighted Mark Method, *Systems Engineering-Theory & Practice*, *21* (2001), 08, pp. 43-48
[33] Kong, L.-P., *et al*., A Study On Heat Transfer Characteristics and Pile Group Influence of Enhanced Heat Transfer Energy Piles, *Journal of Building Engineering*, *24* (2019), July, pp. 100768-100768
[34] Bao, X., *et al.*, Experimental Study on Thermal Response of a PCM Energy Pile in Unsaturated Clay, *Renewable Energy*, *185* (2022), Feb., pp. 790-803
[35] Ziming, C., *et al*., Influence of Backfilling Phase Change Material on Thermal Performance of Precast High-Strength Concrete Energy Pile, *Renewable Energy*, *184* (2022), Jan., pp. 374-390
[36] Liu, H.-L., *et al*., Ultimate Bearing Capacity of Energy Piles in Dry and Saturated Sand, *Acta Geotechnica*, *14* (2019), 3, pp. 869-879

Paper submitted: June 30, 2024
Paper revised: October 1, 2024
Paper accepted: October 11, 2024